Optical Bistability in SOI Microring Resonators

F. De Leonardis[1] and V. M. N. Passaro[2]

[1] Politecnico di Bari, Dipartimento di Ingegneria dell'Ambiente e per lo Sviluppo Sostenibile, viale del Turismo n. 8, 74100 Taranto, Italy
[2] Politecnico di Bari, Dipartimento di Elettrotecnica ed Elettronica, via E. Orabona n. 4, 70125 Bari, Italy

A general modeling of nonlinear effects in silicon-on-insulator optical microring resonators is used to demonstrate optical bistability using either active or passive approach. Stimulated Raman scattering, Kerr effect, two-photon absorption, free carrier absorption and plasma dispersion effect are considered in quasi-CW regime simulations, considering very small radii (from 5 to 20 µm). Results are shown in both cases, i.e. active and passive. These devices could find application for sensing, optical amplification or all-optical memories.

Introduction

While a wide variety of passive optical devices were developed in the 1990's, recent activities have been focused on achieving active functionality, mostly light amplification and generation, in silicon-on-insulator (SOI) waveguides. The most efficient approach for light generation recently investigated, both experimentally and theoretically, is based on Stimulated Raman Scattering (SRS) effect [1]. In fact, as a transmission medium, silicon has much higher nonlinear effects than the commonly used silicon dioxide, in particular the Raman effect. Typically, the other dominant contributions to 3rd order nonlinearity useful for integrated optical devices are Kerr effect and Two-Photon-Absorption (TPA). To the best of our knowledge, devices have been not yet proposed in literature to induce active bistability in SOI technology. In fact, only recently a reduced number of experimental investigations [2-3] have been proposed to induce optical bistability in SOI microring resonators, using a passive approach.

Numerical results: active bistability

In this section, the possibility to realize active optical bistability in SOI microring resonators using SRS is investigated. In our analysis we assume the architecture as sketched in Fig. 1, where the input pump (S_i) is injected in the resonator by means of the evanescent coupling between an external bus waveguide and the microring resonant cavity. In addition, the 3D view of Fig. 1 shows the main geometrical parameters of the architecture, in particular the microring resonator with an external radius R and width W, and the rib waveguide with total height H and slab height H_S. In this device a Stokes wave is excited by SRS mechanism when the pump power is above threshold. By neglecting the walk-off effect between pump and Stokes waves, the power exchange between waves is described by coupled non linear equations in time domain and quasi-CW regime [4]. Thus, a steady-state analysis has been applied, while the condition of SRS threshold leads to neglect the contributions due to Kerr and plasma dispersion effects. In fact, SPM and XPM effects are not excited because they can be considered under threshold, since Raman effect dominates over Kerr effect in SOI technology. Finally, in order to minimize the input pump power at the threshold, we assume both pump and Stokes waves with angular frequencies at the resonance. Therefore, two stable operating points can be derived after applying simple algebra,, i.e. two possible threshold levels for the input pump S_i can be selected to excite SRS in the cavity resonator [4].

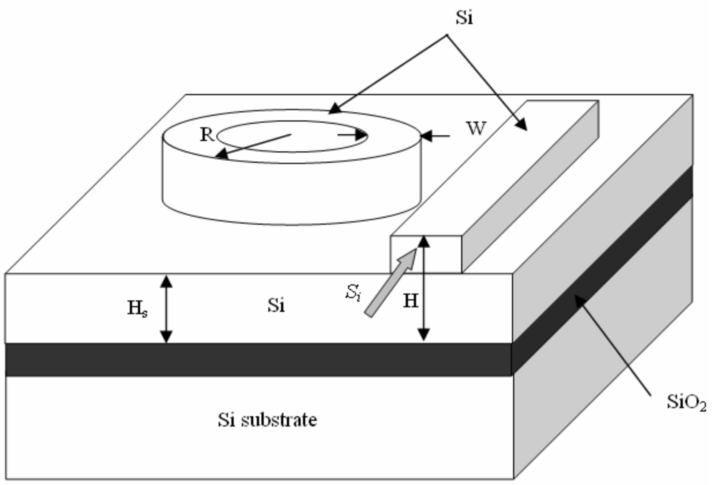

Fig. 1. 3D view of SOI microring resonator, coupled with the bus waveguide.

This pair of values for SRS threshold is influenced by Two Photon Absorption (TPA) and Free Carrier absorption (FCA) effects. Moreover, for a given value of pump coupling factor κ_p^2, the upper threshold value ($P_{th,1}$) increases and the smaller level ($P_{th,2}$) is lower, with decreasing the coupling factor κ_s^2 for the Stokes wave. By contrast, for a given value of κ_s^2, both threshold levels increase with decreasing the coupling factor for the input pump κ_p^2. Fig. 2 shows in logarithmic scale the input threshold pump power as a function of Stokes coupling factor κ_s^2, for different ring radii, assuming TPA coefficient $\beta^{(TPA)} = 0.5$ cm/GW, Raman gain g_R = 10.5 cm/GW, linear loss $\alpha_{loss,p} = \alpha_{loss,s} = \alpha_{loss}$ = 0.6 dB/cm, and recombination effective lifetime τ_{eff} =1 ns.

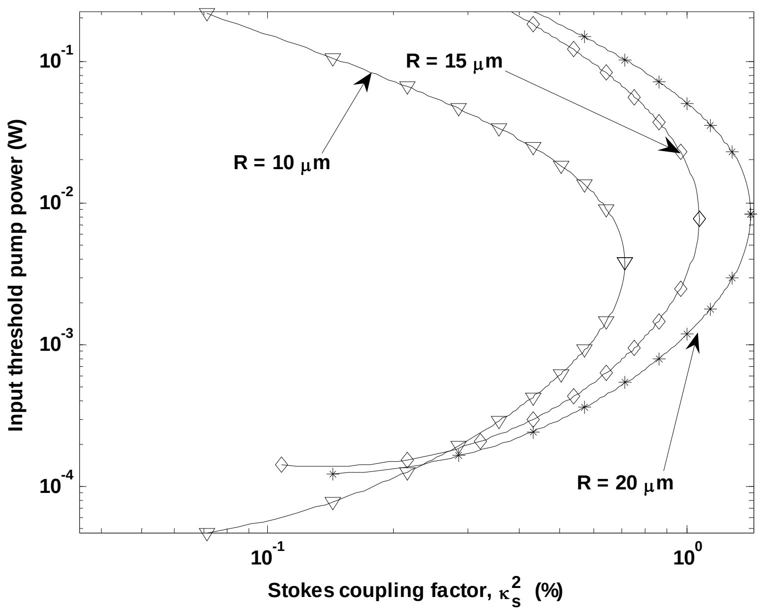

Fig. 2. Input threshold pump power versus Stokes coupling factor for various ring radii.

The calculations of field distributions, effective indices and modal areas have been carried out by full-vectorial finite element method. The plots clearly demonstrate that two values of laser threshold still exist for each ring radius, namely one upper and one smaller. The two arms of the curves in Fig. 2 merge at one limit point. Thus, SRS effect can be excited into the microring cavity in quasi-CW regime only if the coupling factor κ_s^2 is not larger than a critical value, depending on the ring radius. Similar considerations can be outlined by observing Fig. 3, where the input threshold pump power and the external laser efficiency are sketched as a function of Stokes coupling factor κ_s^2 for different Raman gains, assuming α_{loss} = 0.46 cm^{-1} and R = 20 μm. Therefore, active bistability can be achieved in SOI microring resonators.

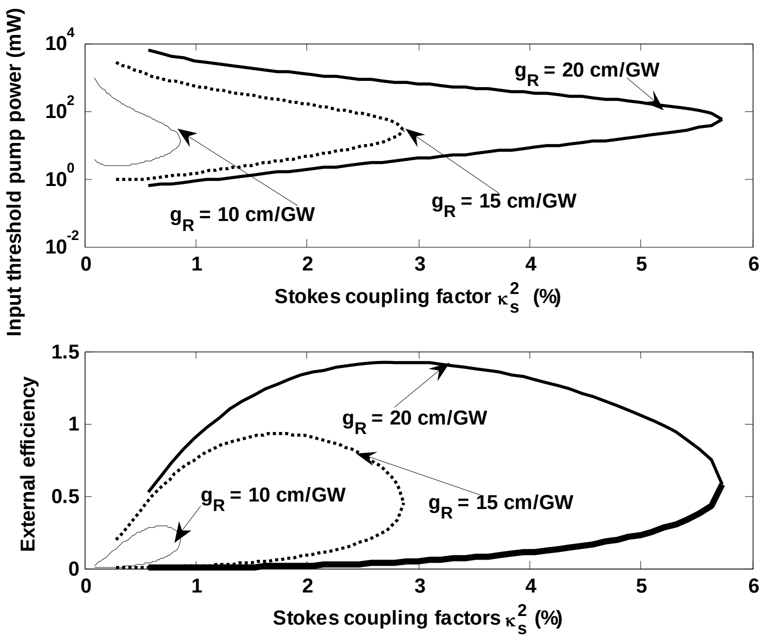

Fig. 3. Input threshold pump power and external efficiency versus Stokes coupling factor, for different values of Raman gain.

Numerical results: passive bistability

As demonstrated in [2], the most direct application of optical bistability is in all-optical memory. This functionality depends on the switching of the output power between two stable states by modulating the input power. The bistability in passive ring resonators can be obtained by exploiting nonlinear effects such as TPA, FCA, Kerr effect and plasma dispersion effect, as it is shown in this section. The relevant mathematical model can be considered as a particular case of the complete equation system in time domain. In Fig. 4 the normalized output power spectra are shown for a microring resonator excited with input powers of 2.5 or 10 mW, by considering a ring radius of 5 μm and a cross section width W = 0.36 μm, H = 0.5 μm, H_s = 0.25 μm. The coupling factor has been assumed equal to 2%. The plot puts into evidence the difference between the spectra in linear operation condition (solid line) and those under influence of the cited nonlinear effects. It is possible to observe that, as the input power is changed from 2.5 to 10 mW, the ring resonance shifts of about 0.1 nm towards larger wavelengths, thereby modifying the ring resonator transmittance, as due to Kerr and plasma dispersion effects in silicon. This resonance shift strongly depends on the circulating optical power inside the ring, which in its turn depends on the wavelength detuning between optical source and shifted resonance. The combined effect of these interrelated mechanisms leads to a passive bistability behaviour, similarly as in [2].

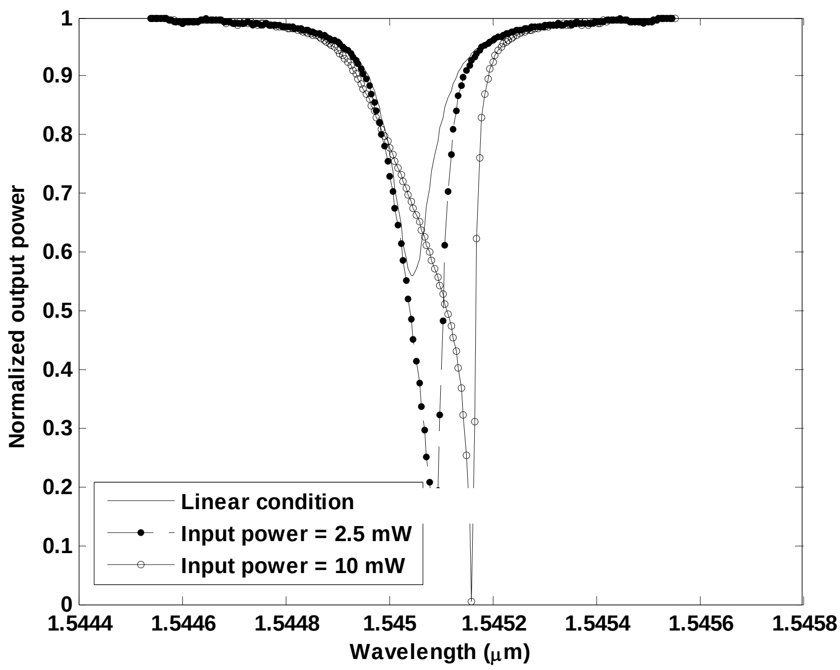

Fig. 4. Normalized output power spectra for different values of input power, as compared with linear case (solid line without markers).

References

[1] O. Boyraz and B. Jalali, "Demonstration of a silicon Raman laser," Opt. Express, vol. 12, 5269-5273, 2004.

[2] R. Almeida and M. Lipson, "Optical bistability on a silicon chip," Opt. Letters, vol. 29, 2387-2389, 2004.

[3] Q. Xu and M. Lipson, "Carrier-induced optical bistability in silicon ring resonators," Opt. Letters, vol. 31, 341-343, 2006.

[4] F. De Leonardis and V.M.N. Passaro, "Modelling of Raman amplification in silicon-on-insulator optical microcavities," New Journal of Physics, vol. 9, n. 25, 2007.